A Study on the Input Circuit of the Contact Modulated Amplifier

By

Nobuyoshi KATO and Jun-ichi IKENOUE

Department of Electronic Engineering

1. Introduction

The contact modulated amplifier is often used to amplify very small d. c. voltage generated by a signal source apparatus, having a low impedance such as a thermopile. In the contact modulated amplifier, d. c. signal voltage to be amplified is converted first into a.c. voltage by a mechanical interrupter and then amplified by a high sensitive a. c. amplifier. Then, the output voltage of the a. c. amplifier is converted into magnified d. c. voltage by means of a phase sensitive rectifier. This type of d. c. amplification has the following advantages :

(1) We can apply magnified signal to the control grid of the amplifying tube on the first stage by using the input transformer having large turn ratio.

(2) We can use an a.c. amplifier which is more stable than a d. c. amplifier.

(3) The noise may be reduced by using the phase sensitive rectification, etc.

However, the secondary voltage of the input transformer of the contact modulated amplifier is a series of damped oscillations since the d. c. signal voltage is periodically interrupted by the mechanical interrupter S as shown in Fig. 1.1. Hence, the design of the input circuit of this amplifier should be treated by the theory of transient phenomena. In this paper, we shall analyze the input circuit of the contact modulated
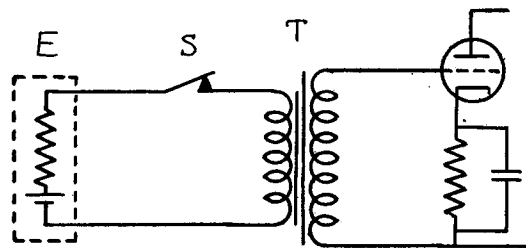

Fig. 1.1.

E : Signal source
S : Interrupter
T : Input transformer

amplifier by the analytical method of interrupted circuits proposed by Prof. S. Hayashi and illustrate the characteristics of the input circuit of this amplifier.

2. Analysis of the Input Circuit of a Contact Modulated Amplifier for the Constant D. C. Signals

Transforming the input circuit of the contact modulated amplifier described above into an equivalent circuit on the primary side of an input transformer, we get the circuit shown in Fig. 2.1.
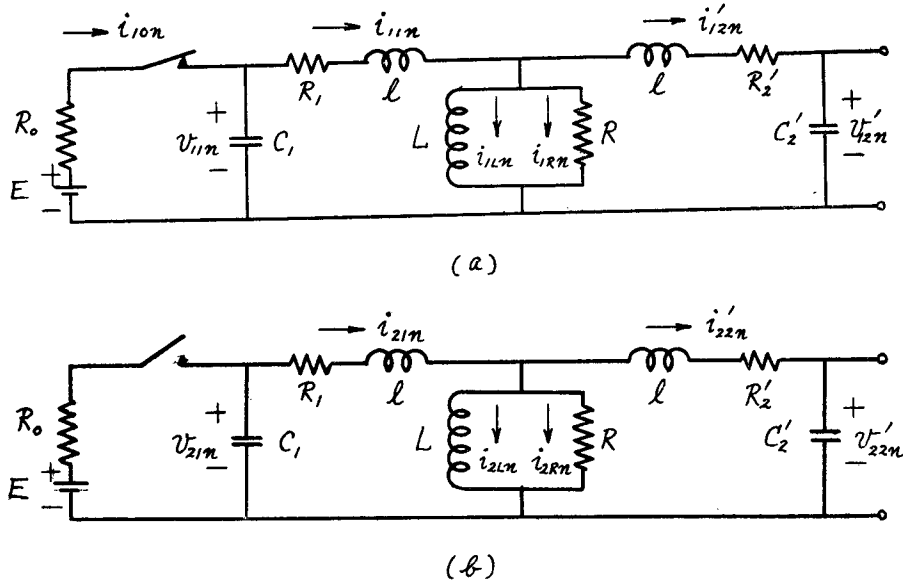

(a)

(b)

Fig. 2.1.

Here we assume that the first circuit mode represents a condition in which the interrupter is closed and the second circuit mode is that in which the interrupter is open. Assuming the notations as shown in the figure, we can easily establish the following circuit equations for the first circuit mode on the n-th stage:

$$
\left.
\begin{aligned}
\left(l\frac{d}{dt}+R_1\right)i_{11n} \quad\quad\quad +L\frac{d}{dt}i_{1Ln} \quad\quad -v_{11n} \quad\quad\quad &=0 \\
\left(l\frac{d}{dt}+R_2'\right)i_{12n}'-L\frac{d}{dt}i_{1Ln} \quad\quad\quad +v_{12n}'&=0 \\
R_0i_{10n} \quad\quad\quad\quad\quad\quad\quad +v_{11n} \quad\quad &=E \\
L\frac{d}{dt}i_{1Ln}-Ri_{1Rn} \quad\quad &=0 \\
-i_{10n} \quad +i_{11n} \quad\quad\quad +C_1\frac{d}{dt}v_{11n} \quad\quad &=0 \\
-i_{12n}' \quad\quad\quad +C_2'\frac{d}{dt}v_{12n}'&=0 \\
i_{11n} \quad -i_{12n}' \quad -i_{1Ln} \quad -i_{1Rn} \quad\quad &=0
\end{aligned}
\right\} \quad (2.1).
$$

Then, eliminating the current components i_{10n} and i_{1Rn} in the above equations, since they do not serve in electromagnetic fluxes, we have the following differential equations:

$$
\left.\begin{aligned}
\left(l\frac{d}{dt}+R_1\right)i_{11n} \qquad\qquad +L\frac{d}{dt}i_{1Ln} \qquad\qquad -v_{11n} \quad &=0 \\
\left(l\frac{d}{dt}+R_2'\right)i_{12n}'-L\frac{d}{dt}i_{1Ln} \qquad\qquad +v_{12n}' &=0 \\
-Ri_{11n} \quad +Ri_{12n}'+\left(L\frac{d}{dt}+R\right)i_{1Ln} \qquad\qquad &=0 \\
i_{11n} \qquad\qquad +\left(C_1\frac{d}{dt}+G_0\right)v_{11n} \quad &=I \\
-i_{12n}' \qquad\qquad +C_2'\frac{d}{dt}v_{12n}' &=0
\end{aligned}\right\} \quad (2.2),
$$

where
$$ I=\frac{E}{R_0} \quad \text{and} \quad G_0=\frac{1}{R_0}. $$

Similarly for the second circuit mode on the n-th stage, we have

$$
\left.\begin{aligned}
\left(l\frac{d}{dt}+R_1\right)i_{21n} \qquad\qquad +L\frac{d}{dt}i_{2Ln} \qquad\qquad -v_{21n} \quad &=0 \\
\left(l\frac{d}{dt}+R_2'\right)i_{22n}'-L\frac{d}{dt}i_{2Ln} \qquad\qquad +v_{22n}' &=0 \\
-Ri_{21n} \quad +Ri_{22n}'+\left(L\frac{d}{dt}+R\right)i_{2Ln} \qquad\qquad &=0 \\
i_{21n} \qquad\qquad +C_1\frac{d}{dt}v_{21n} \quad &=0 \\
-i_{22n}' \qquad\qquad +C_2'\frac{d}{dt}v_{22n}' &=0
\end{aligned}\right\} \quad (2.3).
$$

Driving the interrupter periodically, we can get the first circuit mode from the second circuit mode, and vice versa. In this case the arrangement of the inductances and the capacitances is the same in each circuit mode. Herein, the operational functions corresponding to the transient voltages and currents on the first circuit mode on the n-th stage become as follows:

$$
\begin{pmatrix}
lp+R_1 & 0 & Lp & -1 & 0 \\
0 & lp+R_2' & -Lp & 0 & 1 \\
-R & R & Lp+R & 0 & 0 \\
1 & 0 & 0 & C_1p+G_0 & 0 \\
0 & -1 & 0 & 0 & C_2'p
\end{pmatrix}
\begin{pmatrix}
I_{11n} \\ I_{12n}' \\ I_{1Ln} \\ V_{11n} \\ V_{12n}'
\end{pmatrix}
=p
\begin{pmatrix}
l & 0 & L & 0 & 0 \\
0 & l & -L & 0 & 0 \\
0 & 0 & L & 0 & 0 \\
0 & 0 & 0 & C_1 & 0 \\
0 & 0 & 0 & 0 & C_2'
\end{pmatrix}
\begin{pmatrix}
i_{11n}^{-0} \\ i_{12n}'^{-0} \\ i_{1Ln}^{-0} \\ v_{11n}^{-0} \\ v_{12n}'^{-0}
\end{pmatrix}
+
\begin{pmatrix}
0 \\ 0 \\ 0 \\ I \\ 0
\end{pmatrix}
\quad (2.4),
$$

where the suffix $^{-0}$ expresses the initial value of the first kind. Hence, the transient currents and voltages on the first circuit mode on the n-th stage are evaluated as follows:

$$
\left(\begin{bmatrix} i_{1n} \\ v_{1n} \end{bmatrix}\right)=
\begin{pmatrix} i_{11n} \\ i_{12n}' \\ i_{1Ln} \\ v_{11n} \\ v_{12n}' \end{pmatrix}
=\mathfrak{H}
\begin{pmatrix} I_{11n} \\ I_{12n}' \\ I_{1Ln} \\ V_{11n} \\ V_{12n}' \end{pmatrix}
=[\chi_1(t)]\left(\begin{bmatrix} i_{1n}^{-0} \\ v_{1n}^{-0} \end{bmatrix}\right)+[\varphi_1(t)]
\qquad (2.5),
$$

where

$$\mathfrak{H}^{-1}[\chi_1(t)]=[X_1(p)]=p\begin{pmatrix} lp+R_1 & 0 & Lp & -1 & 0 \\ 0 & lp+R_2' & -Lp & 0 & 1 \\ -R & R & Lp+R & 0 & 0 \\ 1 & 0 & 0 & C_1p+G_0 & 0 \\ 0 & -1 & 0 & 0 & C_2'p \end{pmatrix}^{-1}\begin{pmatrix} l & 0 & L & 0 & 0 \\ 0 & l & -L & 0 & 0 \\ 0 & 0 & L & 0 & 0 \\ 0 & 0 & 0 & C_1 & 0 \\ 0 & 0 & 0 & 0 & C_2' \end{pmatrix}$$

$$=\begin{pmatrix} X_{111} & X_{112} & X_{113} & X_{114} & X_{115} \\ X_{121} & X_{122} & X_{123} & X_{124} & X_{125} \\ X_{131} & X_{132} & X_{133} & X_{134} & X_{135} \\ X_{141} & X_{142} & X_{143} & X_{144} & X_{145} \\ X_{151} & X_{152} & X_{153} & X_{154} & X_{155} \end{pmatrix} \qquad (2.6).$$

The values of X_{111}, X_{112}, $\cdots$ and X_{155} are calculated and tabulated in Table 2.1. Next $[\varphi_1(t)]$ is given by

$$\mathfrak{H}^{-1}[\varphi_1(t)]=[\varPhi_1(p)]=\begin{pmatrix} lp+R_1 & 0 & Lp & -1 & 0 \\ 0 & lp+R_2' & -Lp & 0 & 1 \\ -R & R & Lp+R & 0 & 0 \\ 1 & 0 & 0 & C_1p+G_0 & 0 \\ 0 & -1 & 0 & 0 & C_2'p \end{pmatrix}^{-1}\begin{pmatrix} 0 \\ 0 \\ 0 \\ I \\ 0 \end{pmatrix}=\begin{pmatrix} \varPhi_{11} \\ \varPhi_{12} \\ \varPhi_{13} \\ \varPhi_{14} \\ \varPhi_{15} \end{pmatrix} \quad (2.7).$$

Table 2.1.

$\Delta_1 = l^2L(C_1p+G_0)\,C_2'p^4 + \{Ll(R+R_1+R_2')+l(L+l)\,R\}(C_1p+G_0)\,C_2'p^3$ $\quad + [\{R(R_1+R_2')(L+l)+LR_1R_2'\}(C_1p+G_0)\,C_2'+Ll(C_1p+G_0)+LlC_2'p]\,p^2$ $\quad + [RR_1R_2'(C_1p+G_0)\,C_2'+\{R(l+L)+LR_1\}(C_1p+G_0)+\{R(l+L)+LR_2'\}C_2'p]\,p$ $\quad + \{RR_1(C_1p+G_0)+RR_2'C_2'p+Lp\}+R$
$X_{111} = \dfrac{1}{\Delta_1}\,[l^2L(C_1p+G_0)\,C_2'p^4 + \{R(L+l)+R_2'L\}l(C_1p+G_0)\,C_2'p^3$ $\quad + (RR_2'C_2'+L)\,l(C_1p+G_0)\,p^2 + Rl(C_1p+G_0)\,p]$
$X_{112} = \dfrac{1}{\Delta_1}\,RlL(C_1p+G_0)\,C_2'p^3$
$X_{113} = \dfrac{1}{\Delta_1}\,\{RlL(C_1p+G_0)\,C_2'p^3 + RR_2'L(C_1p+G_0)\,C_2'p^2 + RL(C_1p+G_0)\,p\}$
$X_{114} = \dfrac{1}{\Delta_1}\,[lLC_1C_2'p^4 + \{R(L+l)+R_2'L\}\,C_1C_2'p^3 + (RR_2'C_2'+L)\,C_1p^2 + RC_1p]$
$X_{115} = \dfrac{-1}{\Delta_1}\,RL(C_1p+G_0)\,C_2'p^2$
$X_{121} = \dfrac{1}{\Delta_1}\,RlL(C_1p+G_0)\,C_2'p^3$
$X_{122} = \dfrac{1}{\Delta_1}\,[l^2L(C_1p+G_0)\,C_2'p^4 + \{R(L+l)+R_1L\}\,l(C_1p+G_0)\,C_2'p^3$ $\quad + \{RR_1(C_1p+G_0)+Lp\}\,lC_2'p^2 + RlC_2'p^2]$
$X_{123} = \dfrac{-1}{\Delta_1}\,\{RlL(C_1p+G_0)\,C_2'p^3 + RR_1L(C_1p+G_0)\,C_2'p^2 + RLC_2'p^2\}$
$X_{124} = \dfrac{1}{\Delta_1}\,RLC_1C_2'p^3$

$$X_{125} = \frac{-1}{\Delta_1} [lL(C_1 p + G_0) C_2' p^3 + \{R(L+l)+R_1 L\} (C_1 p + G_0)C_2' p^2$$
$$+ \{RR_1(C_1 p + G_0) + Lp\} C_2' p + RC_2' p]$$

$$X_{131} = \frac{1}{\Delta_1} \{Rl^2(C_1 p + G_0) C_2' p^3 + RR_2' l(C_1 p + G_0) C_2' p^2 + Rl(C_1 p + G_0) p\}$$

$$X_{132} = \frac{-1}{\Delta_1} \{Rl^2(C_1 p + G_0) C_2' p^3 + RR_1 l(C_1 p + G_0) C_2' p^2 + RlC_2' p^2\}$$

$$X_{133} = \frac{1}{\Delta_1} [l^2 L(C_1 p + G_0) C_2' p^4 + (2R + R_1 + R_2') lL(C_1 p + G_0) C_2' p^3$$
$$+ \{(RR_1 + RR_2' + R_1 R_2')(C_1 p + G_0) C_2' + l(C_1 p + G_0) + lC_2' p\} Lp^2$$
$$+ \{(R_1 + R)(C_1 p + G_0) + (R_2' + R) C_2' p\} Lp + Lp$$

$$X_{134} = \frac{1}{\Delta_1} (RlC_1 C_2' p^3 + RR_2' C_1 C_2' p^2 + RC_1 p)$$

$$X_{135} = \frac{1}{\Delta_1} \{Rl(C_1 p + G_0) C_2' p^2 + RR_1(C_1 p + G_0) C_2' p + RC_2' p\}$$

$$X_{141} = \frac{-1}{\Delta_1} [l^2 LC_2' p^4 + \{R(L+l)+R_2' L\} lC_2' p^3 + (R_2' RC_2' + L) lp^2 + Rlp]$$

$$X_{142} = \frac{-1}{\Delta_1} RlLC_2' p^3$$

$$X_{143} = \frac{-1}{\Delta_1} (RlLC_2' p^3 + R_2' RLC_2' p^2 + RLp)$$

$$X_{144} = \frac{1}{\Delta_1} [l^2 LC_1 C_2' p^5 + \{Rl(L+l)+(R+R_1+R_2') lL\}C_1 C_2' p^4$$
$$+ \{R(R_1 + R_2')(L+l) C_2' + lL + R_1 R_2' LC_2'\} C_1 p^3$$
$$+ \{RR_1 R_2' C_2' + R(L+l)+R_1 L\} C_1 p^2 + R_1 RC_1 p]$$

$$X_{145} = \frac{1}{\Delta_1} RLC_2' p^2$$

$$X_{151} = \frac{1}{\Delta_1} RlL(C_1 p + G_0) p^2$$

$$X_{152} = \frac{1}{\Delta_1} [l^2 L(C_1 p + G_0) p^3 + \{R(L+l)+R_1 L\} l(C_1 p + G_0) p^2$$
$$+ \{RR_1(C_1 p + G_0) + Lp\}l p + Rlp]$$

$$X_{153} = \frac{-1}{\Delta_1} \{RlL(C_1 p + G_0) p^2 + RR_1 L(C_1 p + G_0) p + RLp\}$$

$$X_{154} = \frac{1}{\Delta_1} RLC_1 p^2$$

$$X_{155} = \frac{1}{\Delta_1} [l^2 L(C_1 p + G_0) C_2' p^4 + \{Rl(L+l)+(R+R_1+R_2') lL\} (C_1 p + G_0) C_2' p^3$$
$$+ \{R(R_1 + R_2')(L+l)(C_1 p + G_0) + lLp + R_1 R_2' L(C_1 p + G_0)\} C_2' p^2$$
$$+ \{RR_1 R_2'(C_1 p + G_0) + R(L+l) p + R_2' Lp\} C_2' p + R_2' RC_2' p]$$

The values of Φ_{11}, Φ_{12}, $\cdots$ and Φ_{15} are calculated and tabulated in Table 2.2.

Table 2.2.

$$\Phi_{11} = \frac{1}{\Delta_1} [lLC_2'p^3 + \{R(L+l)+LR_2'\} C_2'p^2 + (RR_2'C_2'+L) p+R] I$$

$$\Phi_{12} = \frac{1}{\Delta_1} RLC_2'p^2 I$$

$$\Phi_{13} = \frac{1}{\Delta_1} (RlC_2'p^2 + RR_2'C_2'p + R) I$$

$$\Phi_{14} = \frac{1}{\Delta_1} [l^2LC_2'p^4 + \{lL(2R+R_1+R_2') + l^2R\} C_2'p^3$$
$$+ \{R(R_1+R_2')(L+l) C_2' + R_1R_2'LC_2' + Ll\} p^2$$
$$+ \{RR_1R_2'C_2' + R_1L + R(L+l)\} p + RR_1] I$$

$$\Phi_{15} = \frac{1}{\Delta_1} RLpI$$

Similarly, the transient currents and voltages on the second circuit mode on the n-th stage are given by the elements of the following matrix,

$$\left(\begin{bmatrix} i_{2n} \\ v_{2n} \end{bmatrix}\right) = \mathfrak{H}[X_2(p)]\left(\begin{bmatrix} i_{2n}^{-0} \\ v_{2n}^{-0} \end{bmatrix}\right) = [\chi_2(t)]\left(\begin{bmatrix} i_{2n}^{-0} \\ v_{2n}^{-0} \end{bmatrix}\right) \tag{2.8},$$

where the elements of the matrix $[X_2(p)]$, i.e. X_{211}, X_{212}, $\cdots$ and X_{255}, are obtained by substituting zero for G_0 in the expressions of the corresponding elements of the matrix $[X_1(p)]$.

By virtue of the above two equations, we can readily calculate the transient currents and voltages on any circuit mode for any stage by giving any value to the initial currents and voltages of the first kind. When the interrupter is driven periodically, the durations of the periods of each circuit mode will be constant for all stages. Therefore, let us assume these durations of the periods of each circuit mode as t_1 and t_2 respectively. By iterative application of Eq. (2.5) and (2.8), the initial values of the first kind for the first circuit mode on the n-th stage are expressed as follows:

$$\left(\begin{bmatrix} i_{1n}^{-0} \\ v_{1n}^{-0} \end{bmatrix}\right) = \{[U]-[B_1]\}^{-1}\{[U]-[B_1]^{n-1}\}[\chi_2(t_2)][\varphi_1(t_1)] + [B_1]^{n-1}\left(\begin{bmatrix} i_{11}^{-0} \\ v_{11}^{-0} \end{bmatrix}\right) \tag{2.9},$$

where $[U]$ is the unit matrix and $[B_1] = [\chi_2(t_2)][\chi_1(t_1)]$.

We can easily imagine that the periodically interrupted electric circuit shown in Fig. 2.1 will be stable. Therefore, all characteristic roots of the matrix are smaller than unity.

Hence, we can prove the following equation,

$$\lim_{n \to \infty} [B_1]^{n-1} = 0 \tag{2.10}.$$

By using Eq. (2.10), the initial currents and voltages of the first kind at the number of stage n becomes infinite can be estimated as follows:

$$\lim_{n \to \infty} \left(\begin{bmatrix} i_{1n}^{-0} \\ v_{1n}^{-0} \end{bmatrix} \right) = \{[U]-[B_1]\}^{-1}[\chi_2(t_2)][\varphi_1(t_1)] \qquad (2.11).$$

Similarly, the initial values of the first kind for the second circuit mode on the n-th stage can be estimated as follows:

$$\lim_{n \to \infty} \left(\begin{bmatrix} i_{2n}^{-0} \\ v_{2n}^{-0} \end{bmatrix} \right) = \{[U]-[B_2]\}^{-1}[\varphi_1(t_1)] \qquad (2.12),$$

where $[B_2]=[\chi_1(t_1)][\chi_2(t_2)]$.

Substitution of Eq. (2.11) and (2.12) into Eq. (2.5) and (2.8) gives the transient currents and voltages as the elements of the following matrices:

$$\lim_{n \to \infty} \left(\begin{bmatrix} i_{1n} \\ v_{1n} \end{bmatrix} \right) = [\varphi_1(t)]+[\chi_1(t)]\{[U]-[B_1]\}^{-1}[\chi_2(t_2)][\varphi_1(t_1)] \qquad (2.13),$$

$$\lim_{n \to \infty} \left(\begin{bmatrix} i_{2n} \\ v_{2n} \end{bmatrix} \right) = [\chi_2(t)]\{[U]-[B_2]\}^{-1}[\varphi_1(t_1)] \qquad (2.14).$$

3. Numerical Calculation and the Simple Equivalent Circuit

Next, we shall carry out some numerical calculations of the theoretical formulas derived in the preceding paragraph. Measuring an input transformer, we obtained the following results:

$$L=28.3 \times 10^{-3} H., \quad l=0.722 \times 10^{-3} H., \quad R_1=13.0\Omega.,$$
$$R_2'=4.63\Omega., \qquad R=2460\Omega., \qquad N=29.0.$$

Let us assume now that the interrupter is driven at 800 cycles per second and $t_1=t_2$.

The currents and voltages that are induced by the operation of the interrupter are a series of transient phenomena and the time constants of the transient phenomena are given for the first and second circuit modes respectively by the roots of the following two equations;

$$\Delta_1=0 \qquad (3.1)$$

and

$$\Delta_2=0 \qquad (3.2).$$

While the roots of Eq. (3.1) are dependent on the internal resistance of the signal source, the roots of Eq. (3.2) is inherent in the input transformer. In order to render the voltage across the secondary terminals of the input transformer as high as possible and, at the same time, as precisely sinusoidal as possible, it is necessary to adjust the tuning condenser attached to the terminals of the input transformer so that the number of natural frequencies of the transformer may agree with the number of the interruption frequencies and, at the same time, damping factors of the natural oscillation be reduced as small as possible. We then assume the roots of Eq. (3.2) to be as follows:

$$p = -\alpha_{21} \pm j\omega_{21}, \quad p = -\alpha_{22} \pm j\omega_{22}, \quad p = -\alpha_{23} \tag{3.3}.$$

And we determine the combinations of C_1 and C_2' so that $\omega_{21}/2\pi$ will be equal to 800 cycles per second, and calculate α_{21}, α_{22}, $\omega_{22}/2\pi$ and α_{23} for each combination of C_1 and C_2'. The calculated results are shown in Fig. 3.1. In order to make the damping
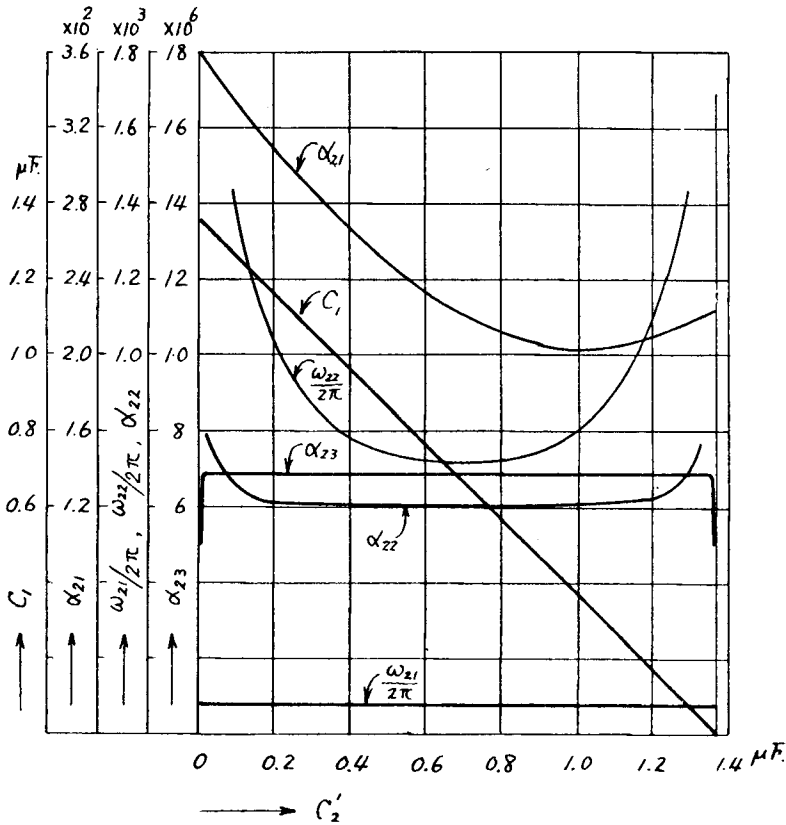

Fig. 3.1.

factor α_{21} minimum, we shall determine from Fig. 3.1 the capacitances of the condensers C_1 and C_2' as follows:

$$C_1 = 0.361 \mu F \quad \text{and} \quad C_2' = 1.015 \mu F.$$

Next, the value of the resistance R_0 is so chosen as to be equal to the magnitude of the impedance viewed from the primary terminals of the input transformer at 800 cycles per second, i. e. 1775 ohms.

Then, substituting the above numerical values into the fundamental formulae already derived, we can finally obtain the actual secondary voltages of the input transformer on the two circuit modes. These voltages are expressed by the following equations:

$$v_{12} = \lim_{n \to \infty} v_{12n} = \lim_{n \to \infty} v'_{12n} \times N = \varepsilon^{-\alpha_{11}t}(-0.46 \cos \omega_{11}t + 13.97 \sin \omega_{11}t)\, E$$
$$+ \varepsilon^{-\alpha_{12}t}(0.05 \cos \omega_{12}t - 0.23 \sin \omega_{12}t)\, E$$
$$- 9.8 \times 10^{-7} \varepsilon^{-\alpha_{13}t}E \tag{3.4}$$

and

$$v_{22} = \lim_{n \to \infty} v_{22n} = \lim_{n \to \infty} v'_{22n} \times N = \varepsilon^{-\alpha_{21}t}(0.47 \cos \omega_{21}t - 13.11 \sin \omega_{21}t)\, E$$
$$+ \varepsilon^{-\alpha_{22}t}(-0.06 \cos \omega_{22}t + 0.22 \sin \omega_{22}t)\, E$$
$$+ 2.7 \times 10^{-5} \varepsilon^{-\alpha_{23}t}E \tag{3.5},$$

where

$$\begin{aligned}
\alpha_{11} &= 4.02 \times 10^{2}, & \omega_{11} &= 5.01 \times 10^{3}, \\
\alpha_{12} &= 6.74 \times 10^{3}, & \omega_{12} &= 5.07 \times 10^{4}, \\
\alpha_{13} &= 6.92 \times 10^{6}, & & \\
\alpha_{21} &= 2.02 \times 10^{2}, & \omega_{21} &= 5.02 \times 10^{3}, \\
\alpha_{22} &= 6.16 \times 10^{3}, & \omega_{22} &= 5.07 \times 10^{4}, \\
\alpha_{23} &= 6.92 \times 10^{6} & &
\end{aligned} \tag{3.6}.$$

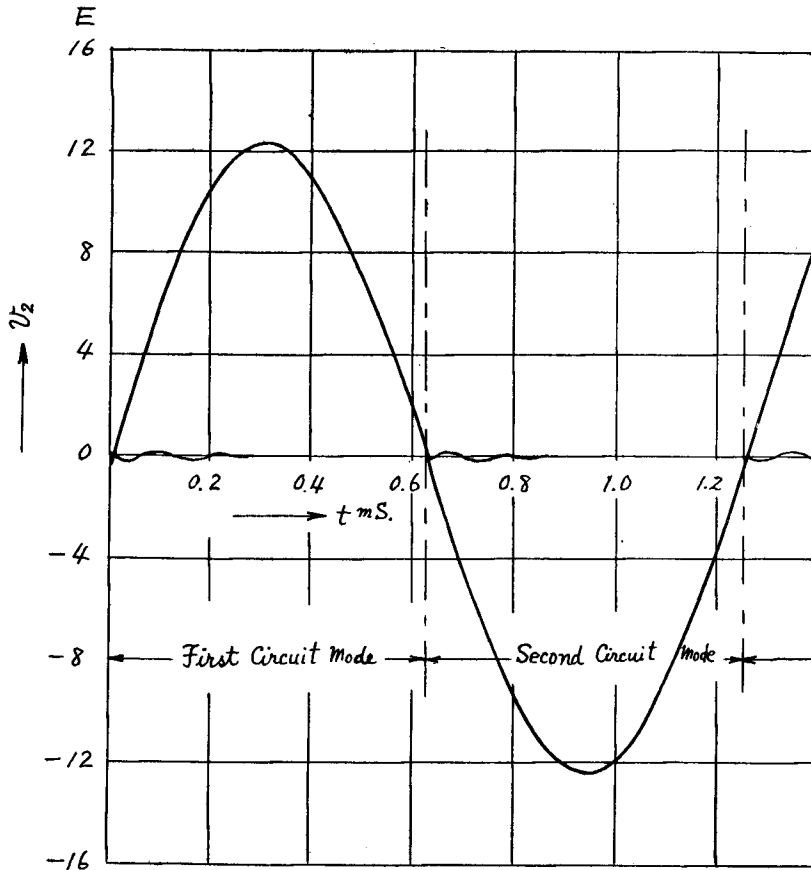Using Eq. (3.4), (3.5) and (3.6), the terminal voltage of the input transformer

Fig. 3.2.

v_2, are plotted in Fig. 3.2. As it is evident from the above equations, the components of voltage waves which have the natural angular frequencies ω_{11} and ω_{21}, each of which corresponds approximately to $2\pi \times 800$, are much greater in comparison than those having the natural angular frequencies ω_{12} and ω_{22} on both circuit modes, i. e. the latters are 2% less than the formers; furthermore, the latters attenuate so rapidly compared with the formers that, when we plot the curves corresponding to v_{12} and v_{22}, the effects of the latters are scarecely recognized. Consequently, in Fig. 3.2, we
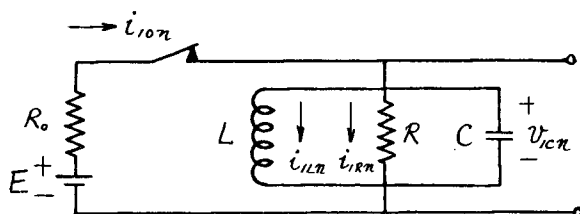

Fig. 3. 3.

plotted curves corresponding to the components of v_{12} and v_{22} with the natural angular frequencies ω_{11} and ω_{21} separately from the other components with the natural angular frequencies ω_{12} and ω_{22}.

When the circuit constants are chosen properly, such a circuit as shown in the above can be approximately replaced by a simple equivalent circuit having single natural frequency as shown in Fig. 3. 3.

On the equivalent circuit as shown in Fig. 3. 3, the similar analysis leads to the following results:

$$\begin{pmatrix} i_{1Ln} \\ v_{1Cn} \end{pmatrix} = \mathfrak{H} \begin{pmatrix} X_{111} & X_{112} \\ X_{121} & X_{122} \end{pmatrix} \begin{pmatrix} i_{1Ln}^{-0} \\ v_{1Cn}^{-0} \end{pmatrix} + \mathfrak{H} \begin{pmatrix} \varPhi_{11} \\ \varPhi_{12} \end{pmatrix} \tag{3.7}$$

and

$$\begin{pmatrix} i_{2Ln} \\ v_{2Cn} \end{pmatrix} = \mathfrak{H} \begin{pmatrix} X_{211} & X_{212} \\ X_{221} & X_{222} \end{pmatrix} \begin{pmatrix} i_{2Ln}^{-0} \\ v_{2Cn}^{-0} \end{pmatrix} \tag{3.8},$$

where the expressions of X_{111}, X_{112}, $\cdots$, $\varPhi_{11}$ and $\varPhi_{12}$ are tabulated in Table 3. 1 and the expressions of X_{211}, X_{212}, $\cdots$ are obtained by substituting zero for G_0 in the expressions of the X_{111}, X_{112}, $\cdots$, respectively. In the above table $G = 1/R$. When the number of stage n extends to infinity, the initial values of the first kind, $i_{1Ln}^{-0} \cdots$ and v_{2Cn}^{-0}, are expressed by the same form as shown in Eq. (2.11) and (2.12). Hence, in the subsequent paragraphs, we shall discuss approximately the input circuit of a contact modulated amplifier by using a simple equivalent circuit.

Table 3. 1.

$\varDelta_1 = LCp^2 + L(G_0 + G) p + 1$
$X_{111} = \dfrac{1}{\varDelta_1} \{LCp^2 + L(G_0 + G) p\}$
$X_{112} = \dfrac{1}{\varDelta_1} Cp$
$X_{121} = \dfrac{-1}{\varDelta_1} Lp$
$X_{122} = \dfrac{1}{\varDelta_1} LCp^2$
$\varPhi_{11} = \dfrac{1}{\varDelta_1} I$
$\varPhi_{12} = \dfrac{1}{\varDelta_1} LpI$

4. Optimum Turn Ratio of the Input Transformer

In Fig. 3. 3, we calculate the change of the

secondary terminal voltage in a case in which the turn ratio of the input transformer is altered by changing the number of turns of primary winding, while the internal resistance of the d. c. signal source R_0 and the number of turns of secondary winding are left constant.

When the signal source is a pure a. c. source and the transformer is resonant to the frequency of the signal, the impedance matching is obtained at a turn ratio by which the resonant impedance of the transformer, viewed from the primary terminal, is equal to R_0. Hence, we shall assume that such a transformer is a standard one and its turn ratio is denoted

Fig. 4.1.

by N_0. Then, the equivalent circuit of the input transformer having the arbitrary turn ratio $N' \times N_0$, when transformed into the primary side of the standard transformer, becomes as shown in Fig. 4. 1.
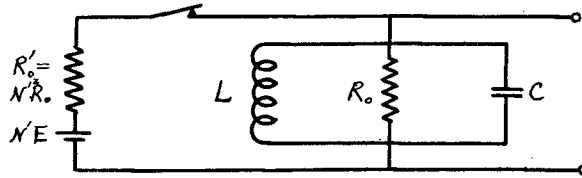
In Fig. 4.1, we assumed the following numerical values,

$$L = 29.05 \times 10^{-3} H , \quad R_0 = 1775 \Omega , \quad C = 1.360 \mu F .$$

$t_1 = t_2$, and the interruption frequency to be equal to 800∿; and we calculated the secondary voltage of the transformer for various values of N' and plotted the curve showing the relation between the fundamentals of the secondary voltage and the value of N' in Fig, 4. 2. From the above figure, it is concluded that the optimum turn ratio is equal to $0.7N_0$ and the optimum amplitude is equal to $0.45E$.
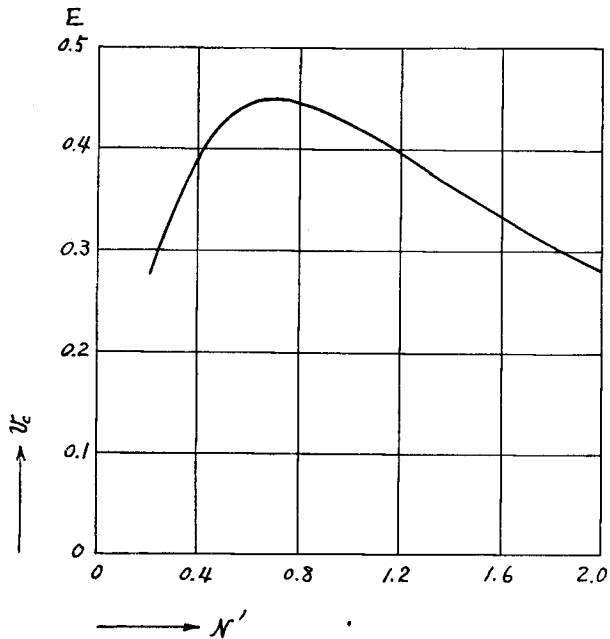
Next, the relation between the harmonic contents of the secondary voltage and the value of N' is shown in
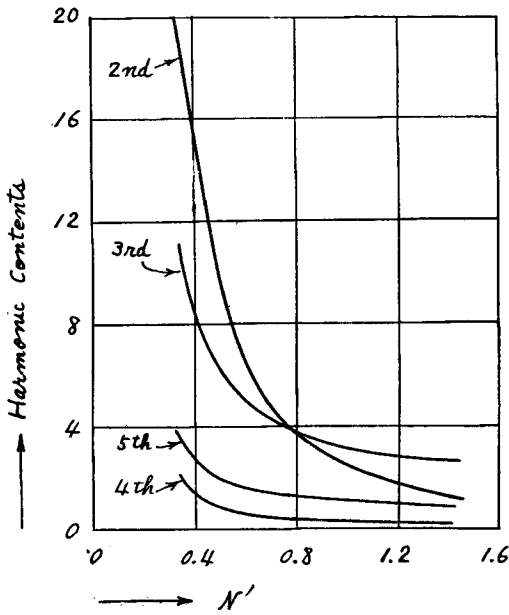

Fig. 4. 2.

Fig. 4.3.

Fig. 4. 3. This figure illustrates that the smaller the value of N', the larger become the harmonic contents.

The above conclusion concerning with the optimum turn ratio has been obtained by the numerical calculation for a particular input transformer; however, it can be proved by further numerical calculations for other arbitrary transformers with different circuit constants that the above conclusion is approximately true in almost all cases. Also, when t_1 is not equal to t_2, the optimum secondary voltage becomes small but the optimum turn ratio is approximately equal to $0.7N_0$.

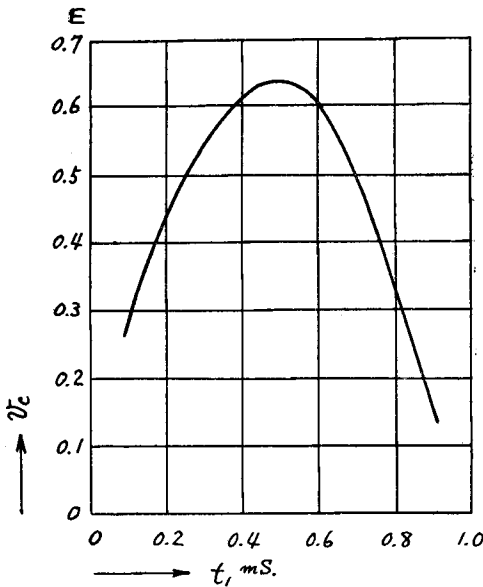## 5. Relation between the Duration of the Closed Period t_1 and the secondary voltage

Fig. 5. 1.

We shall now consider the relation between the duration of the closed period t_1 and the secondary voltage under the assumption that the interruption frequency is equal to the natural frequency of the input transformer.

In Fig. 3. 3, assuming that

$$
\left.
\begin{aligned}
f_0 &= \frac{1}{2\pi} \sqrt{\frac{1}{LC} - \left(\frac{1}{2RC}\right)^2} = 1000\sim \\
R &= 2R_0 \\
Q &= \frac{R}{2\pi f_0 L} = 10
\end{aligned}
\right\} \quad (5.1)
$$

and the interruption frequency is equal to 1000$\sim$, we calculated and plotted in Fig. 5. 1 the curve which shows the relation between t_1 and the secondary

voltage. From this curve, it is shown that such operation as $t_1 = 0.5 \times 10^{-3}$ second, i. e. $t_1 = t_2$, is optimum.

6. Relation between the Interruption Frequency f_i
and the Secondary Voltage

The relation between the interruption frequency f_i and the secondary voltage is discussed under the condition that the natural frequency of the input circuit is a constant value.
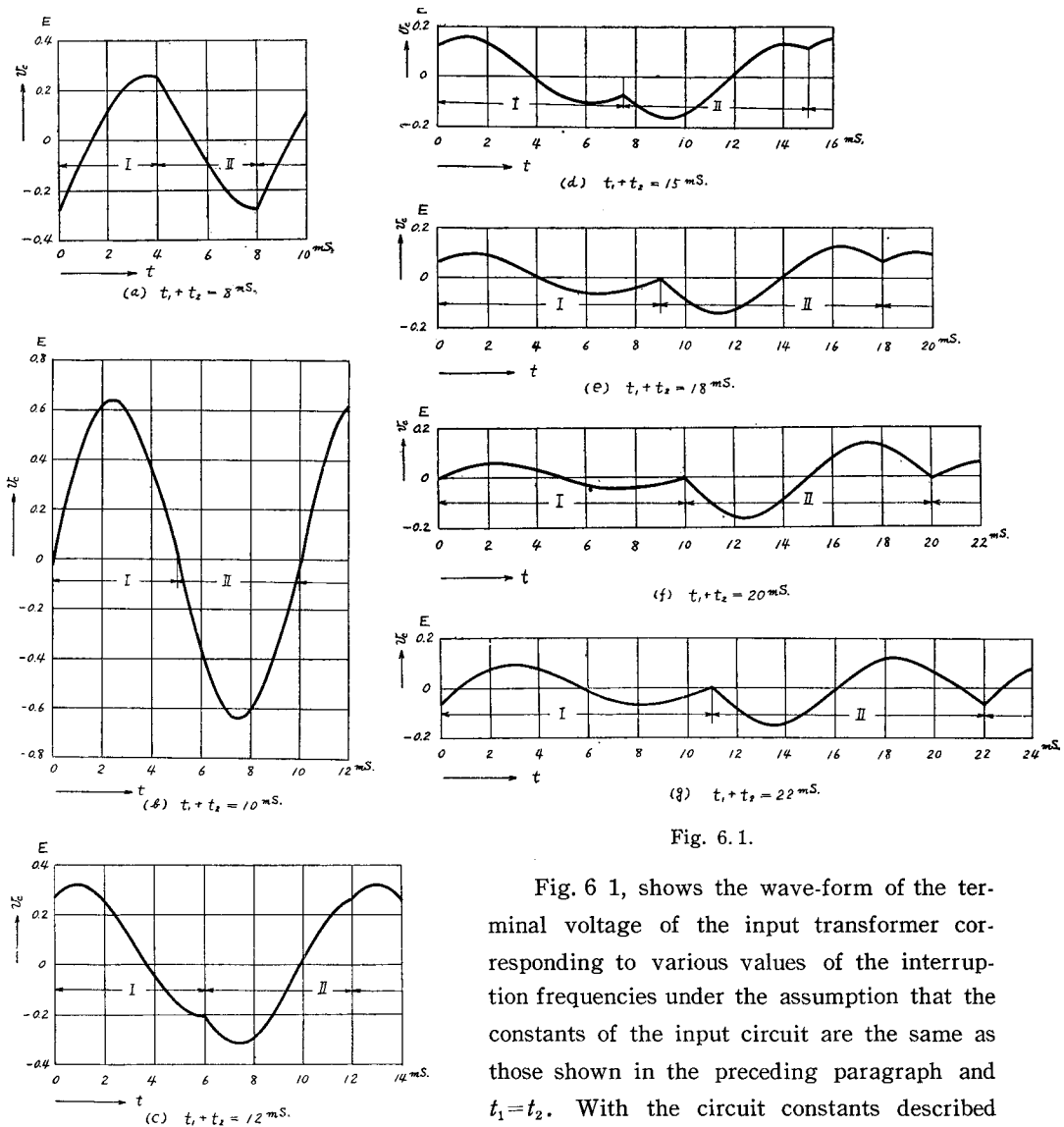

Fig. 6.1.

Fig. 6 1, shows the wave-form of the terminal voltage of the input transformer corresponding to various values of the interruption frequencies under the assumption that the constants of the input circuit are the same as those shown in the preceding paragraph and $t_1 = t_2$. With the circuit constants described

above, t_1' is nearly equal t_2', where t_1' and t_2' respectively are the half-periods of the natural oscillation of the input circuit on the first and the second circuit modes. Consequently, Fig. 6. 1 clearly indicates that a large and sinusoidal secondary voltage occurs under the following conditions :

$$
\left.
\begin{aligned}
t_1 &= (2p+1)\, t_1', \quad p=0,\ 1,\ 2,\ \cdots \\
t_2 &= (2q+1)\, t_2', \quad q=0,\ 1,\ 2,\ \cdots
\end{aligned}
\right\}
\qquad (6.1).
$$

Hence, if we aim to accentuate and amplify the wave having twice frequency of the interruption, it is desirable that the interrupter is driven under the following conditions:

$$t_1 = t_1', \quad t_2 = 3t_2', \qquad\qquad (6.2)$$

and
$$t_1 = 3t_1', \quad t_2 = t_2' \qquad\qquad (6.3).$$

Similarly, when the wave having triple frequency is utilized as the signal to be amplified, the following conditions are suitable :

$$t_1 = t_1', \quad t_2 = 5t_2' \qquad\qquad (6.4),$$

$$t_1 = 3t_1', \quad t_2 = 3t_2' \qquad\qquad (6.5)$$

and
$$t_1 = 5t_1', \quad t_2 = t_2' \qquad\qquad (6.6).$$

Table 6. 1 shows approximate values of the amplitudes of the accentuated waves under the conditions described above. Comparison of the interrupting conditions which produce the same order of a frequency multiplication shows the fact that the output voltage increases with the decrease of t_1.

Table 6. 1.

	Fundamental	2nd harmonics		3rd harmonics		
Interrupting conditions	$t_1=t_1'$ $t_2=t_2'$	$t_1=t_1'$ $t_2=3t_2'$	$t_1=3t_1'$ $t_2=t_2'$	$t_1=t_1'$ $t_2=5t_2'$	$t_1=3t_1'$ $t_2=3t_2'$	$t_1=5t_1'$ $t_2=t_2'$
Output voltages	0.638	0.423	0.260	0.316	0.219	0.166
Percentages for fundamental	100	66.4	40.8	49.5	34.3	26.0

7. Analysis of the Input Circuit of the Contact Modulated Amplifier for Sinusoidal Waves

The contact modulated amplifier can be utilized not only for the amplification of the d. c. voltage but also for the amplification of the extremely low frequency voltage. Hence, we shall carry out an analysis of
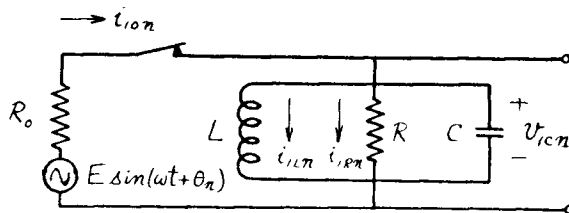

Fig. 7. 1.

the contact modulated amplifier for the sinusoidal signal voltage $E \sin(\omega t + \theta_n)$.

Based on the equivalent circuit shown in Fig. 7.1 and establishing differential equations for the first circuit mode on the n-th stage and then eliminating the current components i_{10n} and i_{1Rn} in the same equations, we have the following differential equations:

$$L \frac{d}{dt} i_{1Ln} \qquad\qquad - v_{1Cn} = 0$$
$$i_{1Ln} + \left(C \frac{d}{dt} + G_0 + G\right) v_{1Cn} = (\cos \theta_n \sin \omega t + \sin \theta_n \cos \omega t) I$$

$$(7.1),$$

where $\qquad\qquad I = \dfrac{E}{R_0}, \quad G_0 = \dfrac{1}{R_0} \quad$ and $\quad G = \dfrac{1}{R}$.

Similarly for the second circuit mode on the n-th stage, we have

$$L \frac{d}{dt} i_{2Ln} \qquad\qquad - v_{2Cn} = 0$$
$$i_{2Ln} + \left(C \frac{d}{dt} + G\right) v_{2Cn} = 0$$

$$(7.2).$$

In the same way as described in paragraph 2, the currents and voltages for the two circuit modes are expressed as follows:

$$\begin{pmatrix} i_{1Ln} \\ v_{1Cn} \end{pmatrix} = \mathfrak{H}[\mathbf{\Phi}_{1n}(p)] + \mathfrak{H}[X_1(p)]\begin{pmatrix} i_{1Ln}^{-0} \\ v_{1Cn}^{-0} \end{pmatrix} = [\varphi_{1n}(t) + [\chi_1(t)]\begin{pmatrix} i_{1Ln}^{-0} \\ v_{1Cn}^{-0} \end{pmatrix} \qquad (7.3)$$

and

$$\begin{pmatrix} i_{2Ln} \\ v_{2Cn} \end{pmatrix} = \mathfrak{H}[X_2(p)]\begin{pmatrix} i_{2Ln}^{-0} \\ v_{2Cn}^{-0} \end{pmatrix} = [\chi_2(t)]\begin{pmatrix} i_{2Ln}^{-0} \\ v_{2Cn}^{-0} \end{pmatrix} \qquad (7.4),$$

where the elements of the matrices $[\mathbf{\Phi}_{1n}(p)]$ and $[X_1(p)]$ are tabulated in Table 7.1, and the elements of the matrix $[X_2(p)]$ are obtained by substituting zero for G_0 in the expressions of the corresponding elements of the matrix $[X_1(p)]$.

Since the time origin is set at the initial instant of each circuit mode in the above equations, θ_n take different values, $\theta_1, \theta_2, \theta_3, \cdots$ for the respective number of the stage, $1, 2, 3, \cdots$. However, after the time T expressed in the following equation (7.5) has elapsed, the phase relation between the interruption and the gignal waves gets back to the initial stage:

$$T = m(t_1 + t_2) = r \frac{2\pi}{\omega} \qquad (7.5),$$

Table 7.1.

$\Delta_1 = LCp^2 + L(G_0 + G)\, p + 1$
$\Phi_{1n} = \dfrac{1}{\Delta_1} \left\{ \dfrac{\omega p}{\omega^2 + p^2} \cos \theta_n + \dfrac{p^2}{\omega^2 + p^2} \sin \theta_n \right\} I$
$\Phi_{2n} = \dfrac{L}{\Delta_1} \left\{ \dfrac{\omega p^2}{\omega^2 + p^2} \cos \theta_n + \dfrac{p^3}{\omega^2 + p^2} \sin \theta_n \right\} I$
$X_{111} = \dfrac{1}{\Delta_1} \{ LCp^2 + L(G_0 + G)\, p \}$
$X_{112} = \dfrac{1}{\Delta_1} Cp$
$X_{121} = \dfrac{-1}{\Delta_1} Lp$
$X_{122} = \dfrac{1}{\Delta_1} LCp^2$

where m and r are the minimum integers satisfying the above relation.
Hence,

$$
\left.
\begin{aligned}
\theta_1 &= \theta_{m+1} = \theta_{2m+1} \cdots = \theta_{l \times m+1} = \cdots \\
\theta_2 &= \theta_{m+2} = \theta_{2m+2} \cdots = \theta_{l \times m+2} = \cdots \\
&\vdots \\
\theta_m &= \theta_{2m} = \theta_{3m} \quad \cdots = \theta_{(l+1)m} = \cdots
\end{aligned}
\right\}
\tag{7.6}.
$$

Consequently, when the number of the stage tends to become larger the initial values of the first kind for each stage are expressed as follows:

$$
\lim_{n \to \infty}
\binom{i_{1L\, l \times m}^{-0}}{v_{1C\, l \times m}^{-0}}
= [B_1]^{m-1}[S_1][\chi_2(t_2)][\varphi_m(t_1)] + [S_1][\chi_2(t_2)][\varphi_{m-1}(t_1)] + \cdots
$$
$$
+ [B_1]^{m-2}[S_1][\chi_2(t_2)][\varphi_1(t_1)]
\tag{7.7}
$$

$$
\lim_{n \to \infty}
\binom{i_{2L\, l \times m}^{-0}}{v_{2C\, l \times m}^{-0}}
= [S_2][\varphi_m(t_1)] + [B_2][S_2][\varphi_{m-1}(t_1)] + \cdots + [B_2]^{m-1}[S_2][\varphi_1(t_1)]
\tag{7.8}
$$

$$
\lim_{n \to \infty}
\binom{i_{1L(l \times m+1)}^{-0}}{v_{1C(l \times m+1)}^{-0}}
= [S_1][\chi_2(t_2)][\varphi_m(t_1)] + [B_1][S_1][\chi_2(t_2)][\varphi_{m-1}(t_1)] + \cdots
$$
$$
+ [B_1]^{m-1}[S_1][\chi_2(t_2)][\varphi_1(t_1)]
\tag{7.9}
$$

$$
\lim_{n \to \infty}
\binom{i_{2L(l \times m+1)}^{-0}}{v_{2C(l \times m+1)}^{-0}}
= [B_2][S_2][\varphi_m(t_1)] + [B_2]^2[S_2][\varphi_{m-1}(t_1)] + \cdots + [S_2][\varphi_1(t_1)]
\tag{7.10}
$$
$$
\vdots
$$

where

$$
[B_1] = [\chi_2(t_2)][\chi_1(t_1)], \quad [B_2] = [\chi_1(t_1)][\chi_2(t_2)],
$$
$$
[S_1] = ([U] - [B_1]^m)^{-1}, \quad [S_2] = ([U] - [B_2]^m)^{-1}.
$$

Substituting the above $2m$ initial values of the first kind into Eq. (7.3) and (7.4), we can obtain the transient currents and voltages for each stage.

8. The Result of Numerical Calculations

Let us assume that the circuit condition is the same as expressed in Eq. (5.1) and $t_1 = t_1'$, $t_2 = t_2'$, where t_1' and t_2', are respectively the half-periods of the natural oscillation of the first and the second circuit modes. The secondary voltage of the transformer, when the sinusoidal voltage characterised by $m = 16$, $r = 1$ and $\theta_1 = 0$ is applied, is calculated by using the analysis discussed in the previous paragraph and are shown in Fig. 8.1. The envelopes of the wave form in the above figure are nearly equal to the envelopes of the 100% amplitude modulated waves, the carrier frequency of which are equal to the interruption frequency and the signal frequency of which are twice the frequency of the applied sinusoidal signal. The form of the envelopes corresponding to the positive half cycle of the signal voltage is equal to the one corresponding to the negative half cycle, but the carrier waves have the phase shift of 180 degrees every half cycle of the signal. Hence, magnifing the voltage shown in the above figure by the carrier frequency amplifier and rectifing the output of it by the phase sensitive detector, we can obtain the magnified sinusoidal voltage
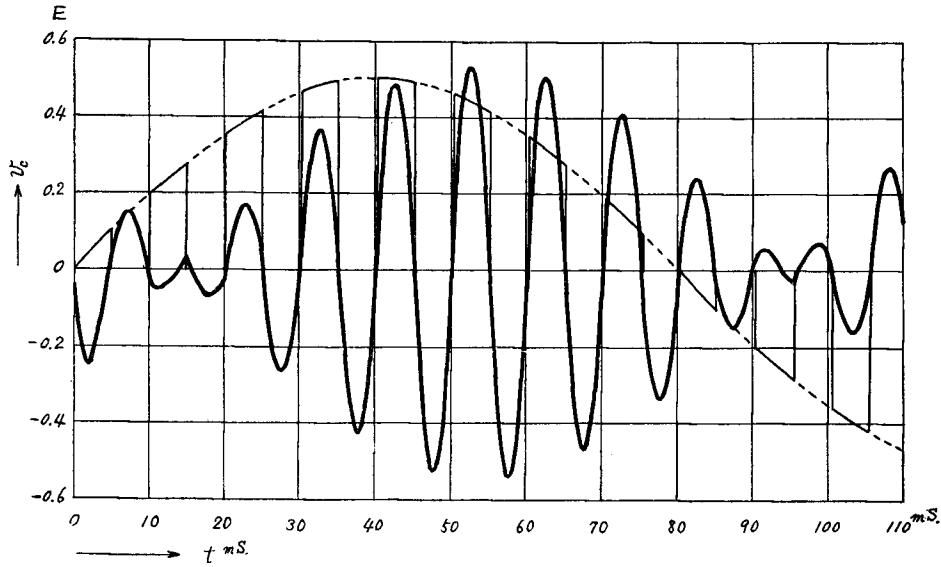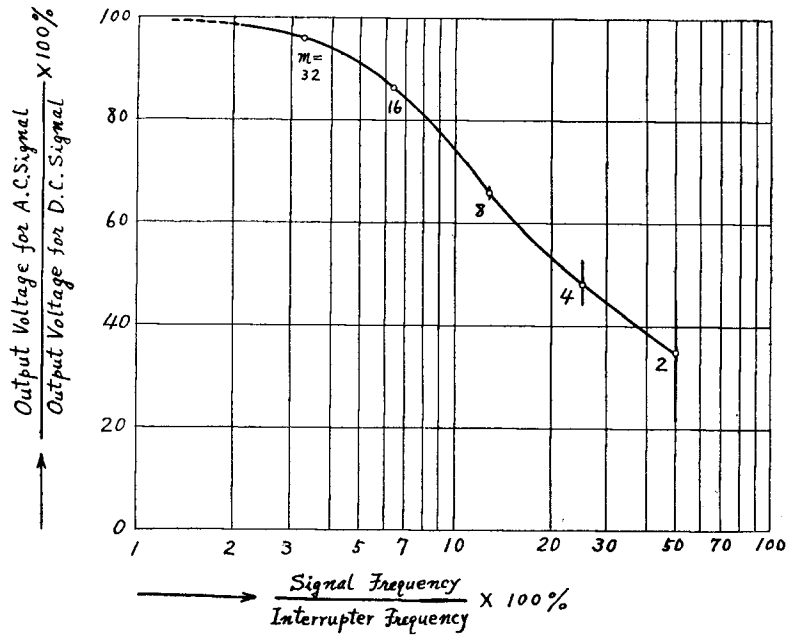
Fig. 8. 1.

Fig. 8. 2.

having the same frequency as the signal voltage. In the above figure, the input sinusoidal wave is shown by the reduced scale of 1/2, however, inspecting the figure, it is noticed that the maximum point of the envelopes lags behind the maximum point of the input wave.

While the value of m is large, for example $m=16$ as shown in the above example, the form of envelopes is independent of the value of θ_1. However, as the value of m becomes smaller, the form of the envelopes is not only influenced more by the value of θ_1, but it is distorted also. Also, as the value of m becomes smaller, the amplitude of the secondary voltage decreases and the phase of the envelopes further lags behind the signal.

Fig. 8.2. shows how the amplitude of the secondaly voltage diminishes as the value of m becomes smaller, by taking as the ordinate the mean value of the maximum amplitudes of the secondary voltage in the half cycle which corresponds to the second circuit mode. The vertical lines at $m=8,$ 4 and 2 indicate the range in which the above mean values vary by the change of the value of θ_1. In the above numerical example, the value of m/r is an integer, but when the value of m/r deviates slightly from an integer, θ_1 varies gradually. Consequently, the above mean values vary gradually in the domains of the vertical lines described above.

9. Conclusion

We have obtained the following results from the above analysis of the input circuit of the contact modulated amplifier by using the analytical method proposed by Dr. S. Hayashi.

1. The simple equivalent circuit of the iunpt circuit of the contact modulated amplifier has been established.

2. The optimum turn ratio of the input transformer, which makes the secondary voltage maximum, is 0.7 time the optimum turn ratio for the sinusoidal signal.

3. The secondary voltage of the input transformer becomes maximum when the duration of the closed time of the interrupter is equal to that of the open time.

4. Also, the secondary voltage becomes maximum and nearly sinusoidal under the condition shown by Eq. (6.1).

5. The contact modulated amplifier can also be utilized for the amplification of the extremely low frequency voltage. In this case, as the ratio of the frequency of the interruption to that of signal voltage becomes smaller, the output of the input transformer diminishes, the phase lag of the envelopes of the output voltage and the distortion of the envelopes increases.

The authers wish to express their sincere thankfulness to Dr. S. Hayashi for his valuable criticism and suggestions.

Reference

S. Hayashi, J.I.E.E. in Japan. **62**, 613 (1942).